Theoretical Investigation on the Electronic and Geometric Structure of GaN2+ and GaN4+

ARTICLE *in* THE JOURNAL OF PHYSICAL CHEMISTRY A · OCTOBER 2007

Impact Factor: 2.69 · DOI: 10.1021/jp074313t · Source: PubMed

3 AUTHORS, INCLUDING:

Demeter Tzeli
National Hellenic Research Foundation
52 PUBLICATIONS **502** CITATIONS
SEE PROFILE

Ioannis D Petsalakis
National Hellenic Research Foundation
142 PUBLICATIONS **1,586** CITATIONS
SEE PROFILE

Theoretical Investigation on the Electronic and Geometric Structure of GaN_2^+ and GaN_4^+

Demeter Tzeli,* Ioannis D. Petsalakis, and Giannoula Theodorakopoulos

Theoretical and Physical Chemistry Institute, National Hellenic Research Foundation, 48 Vassileos Constantinou Avenue, Athens 116 35, Greece

Received: June 4, 2007

The electronic and geometric structures of gallium dinitride cation, GaN_2^+ and gallium tetranitride cation, GaN_4^+ were systematically studied by employing density functional theory (DFT-B3LYP) and perturbation theory (MP2, MP4) in conjunction with large basis sets, (aug-)cc-pVxZ, x = T, Q. A total of 7 structures for GaN_2^+ and 24 for GaN_4^+ were identified, corresponding to minima, transition states, and saddle points. We report geometries and dissociation energies for all the above structures as well as potential energy profiles, potential energy surfaces, and bonding mechanisms for some low-lying electronic states. The calculated dissociation energy (D_e) of the ground state of GaN_2^+, $\tilde{X}^1\Sigma^+$, is 5.6 kcal/mol with respect to $Ga^+(^1S) + N_2(X^1\Sigma_g^+)$ and that of the excited state, $\tilde{a}^3\Pi$, is 24.8 kcal/mol with respect to $Ga^+(^3P) + N_2(X^1\Sigma_g^+)$. The ground state and the first excited minimum of GaN_4^+ are of $^1A_1(C_{2v})$ and $^3B_1(C_{2v})$ symmetry with corresponding D_e of 11.0 and 43.7 kcal/mol with respect to $Ga^+(^1S) + 2N_2(X^1\Sigma_g^+)$ for X^1A_1 and $Ga^+(^3P) + 2N_2(X^1\Sigma_g^+)$ for $^3B_1$.

I. Introduction

Gallium nitrides are semiconducting materials with promising technological applications in microelectronics, nanomaterials, and optics. For example, they form single-crystal nanotubes that have great potential in nanoscale electronics, optoelectronics, and biochemical-sensing applications.[1] The use of GaN and InGaN in the active layer of high-efficiency light emitting diodes enables the emission of amber, green, blue, and ultraviolet light, which makes them ideal for displays and numerous other hi-tech applications.[2] Furthermore, with the use of gallium nitride structures, white light-emitting diodes can be obtained free of electrostatic fields, resulting in dramatic reduction of power consumption with beneficial economic and ecological consequences.[3] As a result, a number of experimental and theoretical studies of the electronic, structural and optical properties of the solid-phase material are reported in the literature.[4] Work on small clusters of GaN either experimental or theoretical is limited, even though information on the geometry and electronic structure of GaN clusters is essential for applications in microelectronics.

Several theoretical studies on Ga_xN_y species have been reported, for example on symmetric molecules, Ga_nN_n ($n = 1-6$[5−8]) as well as on the neutral GaN_2 and GaN_4 species.[9−13] In the case of the cations GaN_2^+ and GaN_4^+, which are the subject of this paper, there are only two studies on GaN_2^+, one devoted to the ground electronic state,[9] the other to the ground and a very highly excited state.[14] As far as we know, there is nothing in the literature on the GaN_4^+ cation.

In the present work the gallium dinitride cation, GaN_2^+, and gallium tetranitride cation, GaN_4^+, were systematically studied using both DFT (B3LYP/LANL2DZ) and MP (MP2, MP4/aug-cc-pV*x*Z, *x* = T, Q) techniques. In total, 7 structures for GaN_2^+ and 34 for GaN_4^+ were determined corresponding to minima, transition states and saddle points. Total energies (E), binding energies (D_e) and geometries (r_e, angles) are reported for the 7 structures of GaN_2^+ and for 24 of GaN_4^+, while the 10 highest transition states and saddle points calculated for GaN_4^+ are provided as Supporting Information. Moreover, vibrational frequencies and potential energy profiles (PEP) and two-dimensional sections of potential energy surfaces (PES) of some low-energy structures of GaN_2^+ and GaN_4^+ are plotted. Finally, the bonding process is discussed.

In section II we describe the computational procedure followed, in section III we discuss the calculation on the triatomic GaN_2^+ cation, in section IV we give our results on GaN_4^+, and, finally, in section V we present some conclusions and comments.

II. Computational Procedure

For the GaN_2^+ cation, the lowest lying singlet and triplet linear ($NNGa^+$ and NGaN) and bent structures were calculated, giving 7 distinct species. For the GaN_4^+ cation, a preliminary sampling of the configuration space and bonding networks was performed using electronic structures of the combining fragments $N_4 + Ga^+$, $N_3 + Ga^+ + N$, $N_2 + GaN_2^+$, $GaN_3^+ + N$, or $GaN_2^+ + 2N$. About 70 structures were checked for stability resulting in 34 singlet and triplet geometry optimized electronic structures of GaN_4^+ at the B3LYP/LANL2DZ level of theory. B3LYP is a DFT functional using Becke's three-parameter gradient corrected functional[15] with the gradient corrected correlation of Lee, Yang, and Parr.[16] The Hay−Wadt LANL2DZ ECP[17] basis set consists of a pseudopotential for the core electrons (up to 3d electrons) of Ga^+ and a double-ζ quality basis set, for the 2 outer electrons of Ga^+, ($4s^24p^0$), and the 7 electrons of N, i.e., (3s3p) → $[2s2p]_{Ga}$ and (10s5p) → $[3s2p]_N$.

Subsequently, all 7 structures of GaN_2^+ and the 17 lowest structures of GaN_4^+ were fully optimized at the MP2/aug-cc-pVTZ level of theory, using second-order perturbation theory and the augmented correlation-consistent basis of Dunning,[18] aug-cc-pVTZ (referred to as atz), i.e., (21s14p10d2f) → $[7s6p4d2f]_{Ga}$ and (11s6p3d2f) → $[5s4p3d2f]_N$, thus involving

* Corresponding author. Fax: +30-210-7273-794. E-mail: dtzeli@eie.gr.

10.1021/jp074313t CCC: $37.00
Published on Web 08/21/2007

TABLE 1: Absolute Energies (hartree), Geometry (Å, deg), Dissociation Energies with Respect of $Ga^+ + 2N$ (D_{e1}) and $Ga^+ + N_2$ (D_{e2}), and Relative Energy ΔE (kcal/mol) of the GaN_2^+ Species

method	$-E$	r_{Ga-N}	r_{N-N}	φ	D_{e1}(BSSE)[a]	D_{e2}(BSSE)[b]	ΔE
Ga−N−N$^+$ ($C_{\infty v}$)				$\tilde{X}^1\Sigma^+$			
B3LYP/LANL2DZ	111.282529	2.647	1.131	180.0	191.4 (189.8)	10.12 (7.40)	0.0
MP2/6-311G+(2df)	2032.360932	2.888	1.113	180.0	235.2 (231.7)	5.39 (4.77)	0.0
MP2/cc-pVTZ	2032.517158	2.797	1.114	180.0	235.1 (232.4)	6.37 (5.37)	0.0
$MP2_{BSSE}$/cc-pVTZ[c]	2032.512849	2.853	1.115	180.0	(232.4)		0.0
$MP2_{BSSE}$/cc-pVTZ[d]	2032.515628	2.870	1.114	180.0		(5.41)	0.0
MP2/aug-cc-pVTZ	2032.526732	2.704	1.114	180.0	237.4 (233.6)	6.74 (5.05)	0.0
$MP2_{BSSE}$/aug-cc-pVTZ[c]	2032.521161	2.859	1.116	180.0	(233.9)		0.0
$MP2_{BSSE}$/aug-cc-pVTZ[d]	2032.524416	2.862	1.114	180.0		(5.29)	0.0
MP4/aug-cc-pVTZ[e]	2032.565866			180.0	229.8 (226.4)	6.73(5.07)	0.0
RCCSD(T)/aug-cc-pVTZ[f]	2032.557809	2.733	1.104	180.0	224.6 (221.4)	6.36 (4.84)	0.0
MP2/cc-pVQZ	2032.624208	2.766	1.110	180.0	241.9 (240.1)	6.57 (5.53)	0.0
$MP2_{BSSE}$/cc-pVQZ[d]	2032.622629	2.835	1.111	180.0		(5.58)	0.0
MP2/aug-cc-pVQZ	2032.630165	2.747	1.111	180.0	243.8 (240.9)	7.39 (5.50)	0.0
$MP2_{BSSE}$/aug-cc-pVQZ[d]	2032.627252	2.829	1.111	180.0		(5.57)	0.0
N−Ga−N$^+$ (C_{2v})				1^1A_1			
B3LYP/LANL2DZ	111.266641	3.530	1.134	18.49	181.4 (180.3)	0.15 (−0.84)	9.97
MP2/aug-cc-pVTZ	2032.518926	3.332	1.115	19.27	232.5 (229.5)	1.84 (0.90)	4.90
$MP2_{BSSE}$/aug-cc-pVTZ[d]	2032.517498	3.456	1.115	18.57		(0.95)	4.34
Ga−N−N$^+$ ($C_{\infty v}$)				$\tilde{a}^3\Pi$			
UB3LYP/LANL2DZ	111.150868	1.832	1.167	180.0	228.4 (225.4)	47.13 (41.59)	82.6
UMP2/cc-pVTZ	2032.360163	2.057	1.097	180.0	255.4 (250.5)	26.67 (23.26)	98.5
$UMP2_{BSSE}$/cc-pVTZ[d]	2032.354891	2.097	1.099	180.0		(23.36)	100.9
UMP2/aug-cc-pVTZ	2032.371195	2.058	1.097	180.0	258.6 (251.9)	27.95 (23.33)	97.6
$UMP2_{BSSE}$/aug-cc-pVTZ[d]	2032.363962	2.093	1.099	180.0		(23.41)	100.7
RCCSD(T)/aug-cc-pVTZ[f]	2032.399650	1.958	1.114	180.0	250.4 (244.2)	32.17 (27.7)	99.2
UMP2/cc-pVQZ	2032.460373	2.035	1.094	180.0	262.4 (259.3)	27.05 (24.67)	102.8
$UMP2_{BSSE}$/cc-pVQZ[d]	2032.456713	2.070	1.096	180.0		(24.75)	104.1
UMP2/aug-cc-pVQZ	2032.468626	2.013	1.093	180.0	265.8 (260.0)	29.39 (24.56)	101.4
$UMP2_{BSSE}$/aug-cc-pVQZ[d]	2032.461260	2.067	1.096	180.0		(24.77)	104.2
N−Ga−N$^+$ (C_{2v})				1^3B_2			
UB3LYP/LANL2DZ	111.116462	2.064	1.226	34.57	206.8 (204.7)	25.54 (22.46)	104.2
UMP2/aug-cc-pVTZ	2032.360543	2.084	1.152	32.10	251.9 (244.8)	21.26 (15.91)	104.3
$UMP2_{BSSE}$/aug-cc-pVTZ[d]	2032.352225	2.116	1.154	31.64		(16.04)	108.1
N−Ga−N$^+$ ($D_{\infty h}$)				$1^3\Sigma_u^+$			
UB3LYP/LANL2DZ	110.916006	1.893	3.786	180.0	81.0 (78.9)		230.0
UMP2/aug-cc-pVTZ	2032.120602	1.870	3.740	180.0	101.3 (94.8)		254.9
N−Ga−N$^+$ ($D_{\infty h}$)				$1^3\Delta_u$			
UB3LYP/LANL2DZ	110.891452	1.891	3.783	180.0	65.6 (63.4)		245.4
UMP2/aug-cc-pVTZ	2032.054830	1.815	3.630	180.0	60.0 (53.5)		296.1
N−Ga−N$^+$ ($D_{\infty h}$)				$^1\Sigma_g^+$			
B3LYP/LANL2DZ	110.856736	1.830	3.660	180.0	−75.8		267.2
UMP2/aug-cc-pVTZ	repulsive						

[a] D_e values of singlet and triplet states calculated with respect to the $Ga^+(^1S)$ and $Ga^+(^3P) + 2N(^4S)$, respectively. [b] D_e values of singlet and triplet states calculated with respect to the $Ga^+(^1S)$ and $Ga^+(^3P) + N_2(^1\Sigma_g^+)$, respectively. [c] MP2-optimized geometry for BSSE correction with respect to Ga + 2N. [d] MP2-optimized geometry for BSSE correction with respect to Ga + N_2. [e] MP4/aug-cc-pVTZ//MP2/aug-cc-pVTZ. [f] T_1 diagnostic = 0.0119 ($\tilde{X}^1\Sigma^+$) and T_1 = 0.0178 ($\tilde{a}^3\Pi$).

TABLE 2: GaN_2^+ Harmonic Frequencies ω_e (cm^{-1}) and IR Intensities (km/mol) at the MP2/aug-cc-pVTZ Level of Theory

	$\tilde{X}^1\Sigma^+$		1^1A_1		$\tilde{a}^3\Pi$		1^3B_2		$1^3\Sigma_u^+$		$1^3\Delta_u$	
	ω_e	IR	ω_e	IR	ω_e	IR	ω_e	IR	ω_e	IR	ω_e	IR
ω_1	95.8	0.0006	123.5i	0.02	238.2	0.3	289.7	1.6	124.9	27.8	97.3	28.2
ω_2	95.8	0.0006	65.1	10.5	285.8	0.05	498.2	12.4	637.8	0	370.3	1312
ω_3	103.5	28.9	2175.0	2.3	289.1	5.9	2494.5	383.0	1592.8	48180	697.2	0
ω_4	2181.2	27.0			3524.5	708.6			1739.0		942.5	7.8

151 (GaN_2^+) and 243 (GaN_4^+) contracted Gaussian functions. For reasons of comparison additional MP2 calculations were performed using a different basis set, the 6-311+G(2df),[19] a split-valence triple-ζ basis set with diffuse and polarization functions for the ground state of GaN_2^+ and for three structures of GaN_4^+. Furthermore, for the two lowest states of the GaN_2^+, MP2 calculation were carried out using Dunning's basis sets[18] cc-pVTZ (referred to as tz), cc-pVQZ (qz), and aug-cc-pVQZ (aqz). The contracted aqz basis set is $[8s7p5d3f2g]_{Ga}$/$[6s5p4d3f2g]_N$, thus consisting of 253 contracted Gaussian functions. The qz basis set was also used for calculations on the two lowest minima of GaN_4^+. Moreover, single point calculations at the fourth-order perturbation theory (MP4SDTQ), MP4/atz//MP2/atz, were carried out for the ground states of both cations and CCSD(T)/atz for the GaN_2^+. In all MP calculations the valence space of GaN_2^+[GaN_4^+] consists of 22[32] e^-, i.e., $3d^{10}(4s4p)^2$ and $2[4]\times 2s^22p^3$ on Ga^+ and N atoms, respectively. In the case of the GaN_2^+ cation, CASSCF (complete active space SCF)/aug-cc-pVTZ calculations were performed by allotting the 13 "valence" electrons in 12 valence orbitals (one 4s + three

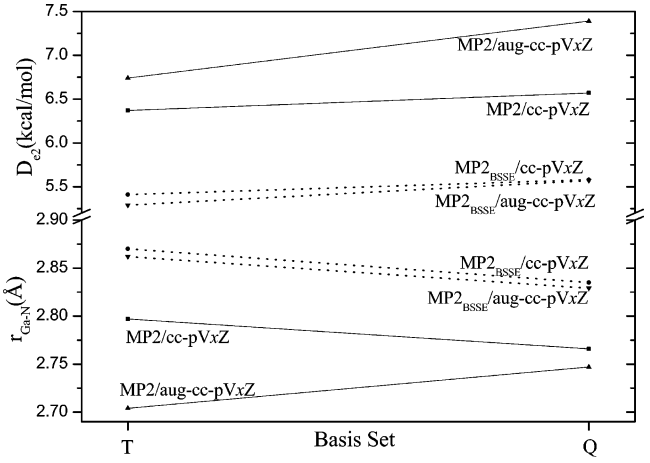

Figure 1. MP2 vdW bond lengths and the dissociation energies correlating to the $Ga^+ + N_2$ (D_{e2}) of the ground state $\tilde{X}^1\Sigma^+$ of GaN_2^+ with respect to basis set size x, x = T (triple), Q (quadruple), and type (augmented or not). The dotted lines correspond to the geometry optimization for the BSSE-corrected energy ($MP2_{BSSE}$).

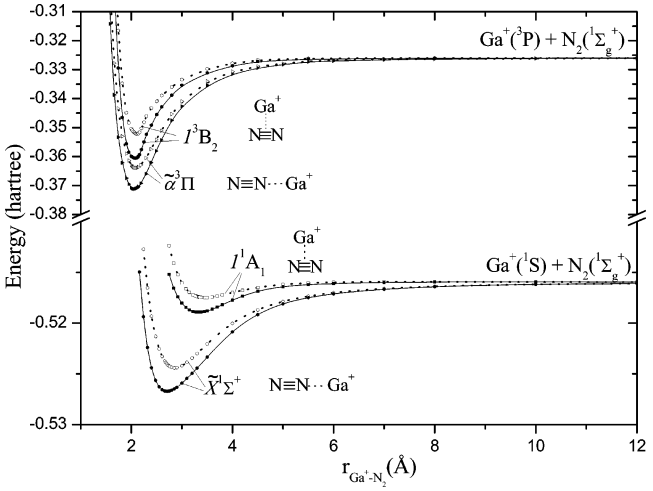

Figure 2. Potential energy curves of the GaN_2^+ cation at the MP2/aug-cc-pVTZ level of theory. The dotted lines correspond to the BSSE-corrected potential energy curves.

4p on Ga, and one 2s + three 2p on N) for 14 electronic structures, to check the MP2 results. Normally, MP2 will only yield the lowest state of a given spin multiplicity within a given symmetry point group. By using CASSCF method, it is possible to determine other singlet or triplet states of different spatial symmetry (e.g.$^{1,3}\Sigma^{\pm}$, $^{1,3}\Pi$ or $^{1,3}\Delta$) that may lie between the lowest singlet ($\tilde{X}^1\Sigma^+$) and triplet state ($\tilde{a}^3\Pi$) of GaN_2^+ calculated by MP2. In general, CASSCF is not sufficient for describing electron correlation effects; however, for the present purposes it is considered to be appropriate.

For all structures at all levels of theory the basis set superposition error (BSSE) was estimated through the counterpoise technique,[20] because BSSE corrections are important in van der Waals systems[21] such as most of the structures studied here. The BSSE was calculated for the fragments with respect to which the particular D_e is reported. For example the BSSE for D_e with respect to $Ga^+ + N_2$ was calculated with respect to these two species and the BSSE for D_e with respect to $Ga^+ +$ 2N was calculated with respect to these three species. For the four lowest electronic states of GaN_2^+ the MP2 geometry was optimized for the BSSE-corrected energy, i.e., $MP2_{BSSE}$.

Finally, there are no size nonextensivity problems in the plotting of the potential energy profiles of GaN_2^+ and GaN_4^+, with the relevant error being less than 0.2 mh.

All MP calculations were performed using the Gaussian 03 program package,[22] and the CCSD(T) and CASSCF calculations were done using MOLPRO 2006.1.[23]

III. GaN_2^+

We calculated seven structures, six minima ($\tilde{X}^1\Sigma^+$, $\tilde{a}^3\Pi$, 1^3B_2, $1^3\Sigma_u^+$, $1^3\Delta_u$ and $^1\Sigma_g^+$), and one transition state (1^1A_1) of the GaN_2^+ cation. Total energies (E), geometries (r_e, angles) and dissociation energies with respect to the $Ga^+(^1S$ or $^3P) + 2N(^4S)$ (D_{e1}) and $Ga^+(^1S$ or $^3P) + N_2(X^1\Sigma_g^+)$ (D_{e2}), calculated with different methods, and/or basis sets, are presented in Table 1. Table 2 gives the corresponding harmonic vibrational frequencies and IR intensities at the MP2/atz level of theory. The variation of the Ga−N bond length and the dissociation energy of the ground state $\tilde{X}^1\Sigma^+$ with respect to $Ga^+ + N_2$ with basis set size and type is given pictorially in Figure 1. In Figure 2 the optimized potential energy profiles (PEPs) of four structures of GaN_2^+ have been plotted along the stretching motion of $Ga^+\cdots N_2$ correlating with the limits $Ga^+(^1S$ or $^3P) + N_2(X^1\Sigma_g^+)$ for the singlet or the triplet states, respectively. In addition, the corresponding BSSE-optimized PEPs have been also plotted (dotted lines in Figure 2). The optimized two-dimensional section of potential energy surface (PES) of the lowest singlet electronic state of GaN_2^+ is plotted in Figure 3. The potential energy profile of the lowest triplet electronic state is depicted in Figure 4.

The ground state of GaN_2^+ cation, $\tilde{X}^1\Sigma^+$, is a linear van der Waals (vdW) system, consisting of the ground state $N_2(X^1\Sigma_g^+)$, which has a triple bond $\sigma^2\pi^2\pi^2$, interacting via a σ vdW bond with $Ga^+(^1S)$, i.e., N≡N···Ga^+. Both natural and Mulliken population analyses show practically no charge transfer. Our best geometry at $MP2_{BSSE}$/aqz level (MP2/aqz geometry, which is optimized for the BSSE-corrected energy) is $r_{Ga-N} = 2.829$ and $r_{N-N} = 1.111$ Å. Comparing the results obtained with different basis sets (see Table 1, Figure 1) we observe that augmentation of the basis set with diffuse functions (aug-) results in shorter vdW bond length compared with the same quality nonaugmented basis set. However, the vdW bond length is increased for both augmented and nonaugmented basis sets when the geometry is optimized for the BSSE-corrected energy, with the difference between r_{Ga-N} of the two kinds of basis sets greatly decreased. So, in quadruple basis sets and after optimizing the geometry for the BSSE-corrected energy, the r_{Ga-N} distances become very similar for the MP2/qz and MP2/aqz level, 2.835 and 2.829 Å, respectively, whereas the r_{N-N} value remains the same at all levels of theory (Table 1). The B3LYP method gives a shorter r_{Ga-N} by 0.2 Å compared to the MP2 values.

Comparing the D_{e2} values, which is the binding energy of $\tilde{X}^1\Sigma^+$ with respect to $Ga^+(^1S) + N_2(X^1\Sigma_g^+)$, obtained using different basis sets and methods (cf. Table 1), we observe that the B3LYP/LANL2DZ compared to the results of the MP and CC methods, overestimates D_{e2}, giving D_{e2}(BSSE) = 10.12 (7.40) kcal/mol, where the number in parentheses indicates the BSSE-corrected value. In general, the D_{e2} value obtained by the MP method without BSSE correction is larger in an augmented basis set than in the corresponding nonaugmented one, but the BSSE correction greatly reduces this difference in both T and Q basis sets (see Figure 1). Practically, there are only small variations in D_e when the BSSE is taken into account in all basis sets. At the $MP2_{BSSE}$/cc-pVQZ and $MP2_{BSSE}$/aug-cc-pVQZ levels of theory (optimizing the geometry for the BSSE-corrected energy), D_{e2} is 5.6 kcal/mol. The MP4/atz//

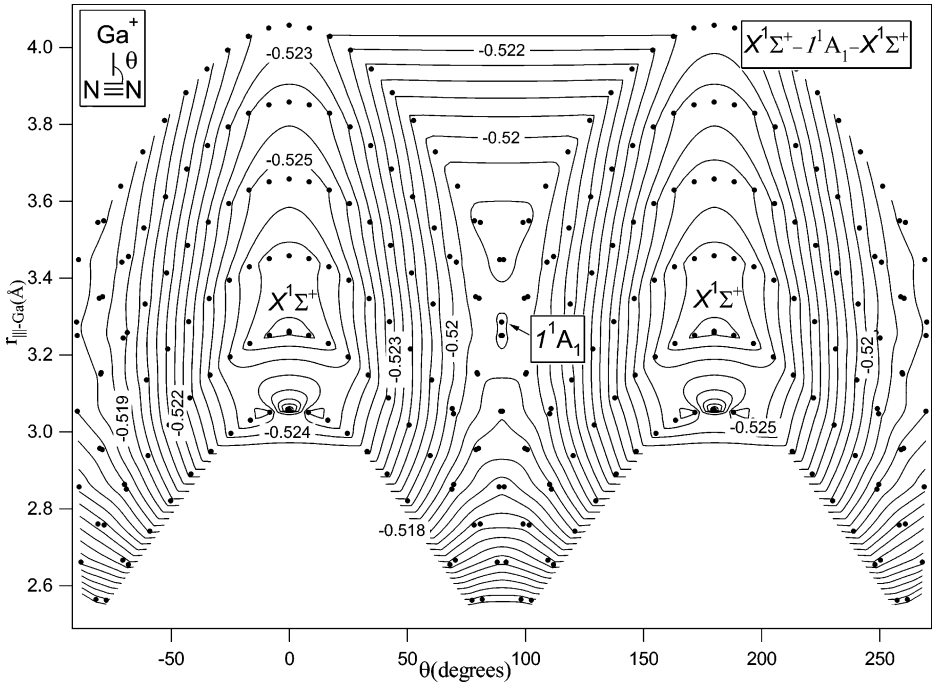

Figure 3. Potential energy surface of $\tilde{X}^1\Sigma^+$ as a function of the Ga−||| distance (||| is the middle of triple bond N_2) and the θ angle represented by contour lines equally spaced by 0.0005 hartree at the MP2/aug-cc-pVTZ level of theory. The contour lines were drawn on the basis of the data calculated at the coordinates represented by the filled circles. (1^1A_1 is the transition state connecting two equivalent $\tilde{X}^1\Sigma^+$ minima.)

MP2/atz D_{e2} value is the same with the corresponding MP2/atz, indicating that the higher order of perturbation does not contribute significantly. Moreover, the CCSD(T)/atz D_{e2} value is very similar to the MP2 result, being only 0.2 kcal/mol smaller than the corresponding MP2/atz (T_1 diagnostic is rather small 0.0119).

A comparison of the optimized PEP (solid) and the BSSE-optimized PEP (open circles in Figure 2) of the $\tilde{X}^1\Sigma^+$ state of GaN_2^+, along the stretching motion of $Ga^+\cdots N_2$ correlating with the limits $Ga^+(^1S) + N_2(X^1\Sigma_g^+)$, shows that the effect of BSSE on the PEP is the increase of the equilibrium bond length r_{Ga-N} by 0.16 Å and the decrease of the well depth by 1.4 kcal/mol, whereas the shapes of the PEP and BSSE-PEP are similar.

Previous calculations on the ground state of GaN_2^+ have been reported in two studies, one employing DFT(GGA)/DNP+d[9] and the other employing the DFT(B3LYP), MP2, and CCD methods combined with the relativistic effective core potentials for the core electrons of Ga^+ and valence Gaussian basis sets for the $3d^{10}4s^24p^1$ of Ga and the N atom.[14] At the DFT/DNP+d level the state is reported to be quasi linear ($\varphi = 178°$) with $r_{GaN} = 2.99$ Å and $D_{e2} = 4.16$ kcal/mol.[9] In ref 14 their B3LYP method gives $r_{GaN} = 2.730$ Å. Their corresponding MP2 and CCD values are 2.699 and 2.762 Å. These values are shorter than our best value of 2.829 Å for the Ga−N equilibrium bond length at the $MP2_{BSSE}$/aqz level of theory.

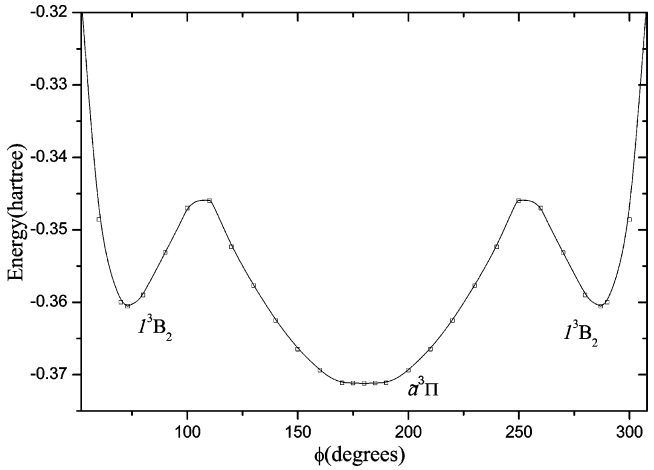

Figure 4. Optimized potential energy profile of the GaN_2^+ $\tilde{a}^3\Pi - 1^3B_2$ with respect to the φ angle.

The lowest energy bent structure of GaN_2^+ has $^1A_1$ symmetry and it is also a vdW structure with a $Ga^+(^1S)$ cation interacting with the triple bond of $N_2(X^1\Sigma_g^+)$ forming a T-shaped molecule. It is the transition state (one imaginary frequency, cf. Table 2) between two equivalent minima at the ground state, $\tilde{X}^1\Sigma^+$, i.e.,

$$\begin{array}{c} Ga^+ \\ Ga^{+}\cdots N{\equiv}N \leftarrow \ \vdots \ \rightarrow N{\equiv}N\cdots Ga^+ \\ N \equiv N \end{array}$$

with a barrier of 4.3 kcal/mol. Note that the B3LYP/LANL2DZ method overestimates significantly the barrier to 10.0 kcal/mol, about twice the MP2 value. The optimized two-dimensional potential energy surface between the two $\tilde{X}^1\Sigma^+$ minima and their transition state 1^1A_1 is plotted in Figure 3, at the MP2/atz level, where the contours are discontinued in the region of the PES where there are no calculated points. As seen in Table 1 the dissociation energy of 1^1A_1 (D_{e2}) with respect to $Ga^+ + N_2$ is only 1.84(0.95) kcal/mol, the distance between Ga^+ and the middle of the N≡N triple bond is rather large 3.285(3.411) Å and the angle φ_{NGaN} is 19.3(18.6)° at the $MP2(MP2_{BSSE})$/atz level of theory. Again, the calculations show that there is practically no charge transfer from N≡N to Ga^+.

The first excited state of GaN_2^+ calculated here is a linear triplet state $\tilde{a}^3\Pi$ correlating with 2 $N(^4S) + Ga^+(^3P$, first excited state). The N atoms form a $X^1\Sigma_g^+$ with a triple bond $\sigma^2\pi^2\pi^2$ and Ga^+ is connected to N_2 with a σ^1 (which is formed between the empty $4p_z$ orbital of Ga and the $2s^2$ orbital of the adjacent N, where the first one gains about 0.1 e^-) and a π^1 (which is formed between the $4p_y^1$ orbital of the Ga^+ and the π_y^2 orbital) of N_2, i.e., $\overline{Ga^+\cdots N{\equiv}N}$. The natural population analysis for this

structure gives Ga^+: $4s^{1.00}4p_z^{0.11}4p_x^0 4p_y^{0.92}$ indicating a small charge transfer from $p_y(Ga^+)$ to $\pi_y(N_2)$ and a back-donation from $\sigma(N_2)$ to $p_z(Ga^+)$. The middle N atom gains about 0.3 e^- and the other N loses ~0.3 e^-.

The reaction energy of $GaN_2^+(\tilde{a}^3\Pi) \rightarrow Ga^+(^3P) + N_2(X^1\Sigma_g^+)$ is $D_{e2} = 24.8$ kcal/mol, at the $MP2_{BSSE}$/aqz level of theory, (cf. Table 1, Figure 2), and the bond distances are $r_{Ga-N} = 2.067$ and $r_{N-N} = 1.096$ Å. The spin contamination of the UMP2 calculation is very small with $\langle S^2 \rangle = 2.01$ instead of 2. The $\tilde{a}^3\Pi$ minimum can also be considered as made of GaN^+ ($^4\Pi$, sixth excited state of GaN^+ [7]) + $N(^4S)$. The N_2 of this structure has shorter r_{N-N} by about 0.01 Å than the free N_2 molecule. As shown in Figure 2 the shapes of the PEP and BSSE-PEP of the $\tilde{a}^3\Pi$ state are very similar, the latter curve having a longer r_e bond length by 0.03 Å and a less deep well by 0.9 kcal/mol at the MP2/atz level.

The triangular 1^3B_2 structure contrary to 1^1A_1 is a minimum and $Ga^+(^3P)$ interacts with the triple N≡N bond of N_2, with a binding energy of 16.0 kcal/mol at the $MP2_{BSSE}$/atz level; cf. Table 1. The distance between Ga^+ and the middle of the triple bond ($r_{Ga-|||}$) and the angle φ_{NGaN} are 2.036 Å and 31.6°, respectively. The 1^3B_2 structure belongs to the surface of the $\tilde{a}^3\Pi$ state and lies at 7.4 kcal/mol above $\tilde{a}^3\Pi$ with a barrier of 9 kcal/mol along the path to the linear structure. The MP2/atz potential energy profile of the lowest triplet electronic state of GaN_2^+ is depicted in Figure 4.

The frequency of the N≡N stretching mode is 2186.2 cm^{-1} in the free N_2 molecule at MP2/atz level. In the $\tilde{X}^1\Sigma^+$and $\tilde{A}^1A_1$ structures the corresponding frequencies are red-shifted only by 5 and 11 cm^{-1} as a result of the formation of the vdW bond (see Table 2). On the contrary the $\tilde{a}^3\Pi$ and 1^3B_2 structures exhibit a large blue shift of 1338 and 308 cm^{-1}, respectively, because the Ga^+-N bond is short and not a vdW bond, so the N_2 is more rigid and cannot stretch freely. That is why, in the case of the linear $\tilde{a}^3\Pi$, the frequency of the stretching mode is increased considerably.

The last two minima, $^3\Sigma_u^+$ and $^3\Delta_u$, listed in Table 1, correspond to linear symmetric structures, $N-Ga-N^+$, with bond distances $r_{Ga-N} = 1.870$ and 1.815 Å, respectively. Two of the three atoms are excited, i.e., $Ga^+(^3P) + N(^4S) + N(^2D)$, and BSSE-corrected binding energies, with respect to them are 170.1 and 128.8 kcal/mol, respectively. Finally, the lowest lying linear symmetric singlet $N-Ga-N^+$ state, $^1\Sigma_g^+$, calculated at 267 kcal/mol above the ground state is bound at the B3LYP/LANL2DZ level but repulsive at the MP2/atz level and unbound with respect to the ground state atoms $Ga^+(^1S) + 2N(^4S)$. In ref 14 this singlet $NGaN^+$ $^1\Sigma_g^+$ was also calculated along with the ground state.

Comparing our results on the GaN_2^+ cation at the MP2/atz level with B3LYP/LANL2DZ, which is a DFT method with a small basis set, we observe a fair agreement on the geometry (the largest difference being less than 11%) and on the calculated D_e with respect to the three separated atoms limit. But in the case of D_{e2} with respect to the $Ga^+ + N_2$ the difference between the two methods is large, as for example, for the case of 1^1A_1, where the BSSE-corrected MP2 method finds this state bound with respect to $Ga^+ + N_2$ products by 1 kcal/mol and the DFT_{BSSE} unbound by 0.8 kcal/mol, but given that the bond is weak, the difference is acceptable. A larger difference is found in the calculated D_{e2} for $\tilde{a}^3\Pi$, where the $MP2_{BSSE}$ value is 23.3 and the DFT_{BSSE} value is 41.6 kcal/mol. Moreover, differences are found in the relative energy of some structures as, for example, between the $\tilde{X}^1\Sigma^+$ and 1^1A_1 structures, resulting in a value for the barrier height for the isomerization $\tilde{X}^1\Sigma^+ \rightarrow 1^1A_1 \rightarrow \tilde{X}^1\Sigma^+$, which is twice the MP2 value.

IV. GaN_4^+

In the present work we have calculated 34 structures, 12 minima, and 22 transition states or saddle points of the GaN_4^+ cation. The 10 highest transition states and saddle points are given as Supporting Information. The geometries of the remaining 24 structures at different levels of treatment are summarized in Figure 5. For convenience the structures have been labeled by three symbols, the first indicating the spin multiplicity (1 or 3), the second the kind of structure, i.e., whether it is a minimum (m) or a saddle point (s), and the third the energy rank of the structure; for instance, 1s2 means 1 = singlet, s = (saddle point), and 2 = second lowest energy structure. In Table 3 total energies (E), dissociation energies D_{e1} with respect to $Ga^+(^1S$ or $^3P) + 4N(^4S)$, D_{e1} with respect to $Ga^+(^1S)/Ga^+(^3P) + 2N_2(X^1\Sigma_g^+)$, and D_{e3} with respect to $GaN_2^+ + N_2(X^1\Sigma_g^+)$ or $Ga^+ + N_4$ as appropriate in each case (see discussion below) are presented. Table 4 gives vibrational frequencies and IR intensities calculated for the six lowest lying singlet and eight lowest lying triplet structures of GaN_4^+. Figures 6−10 depict the optimized potential energy profiles with respect to $Ga^+ + 2N_2$ or $GaN_2^+ + N_2$ and the optimized two-dimensional potential energy surfaces between the two lowest minima (1m1 and 3m3) and their two transition states (1s2 and 3s4).

The ground state of GaN_4^+, $\tilde{X}^1A_1$, is a triangular structure (Figure 5a, 1m1), which may be considered as either having two $N_2(X^1\Sigma_g^+)$ interacting with $Ga^+(^1S)$ via two van der Waals (vdW) bonds or consisting of a $GaN_2^+(\tilde{X}^1\Sigma^+)$ and a $N_2(X^1\Sigma_g^+)$ interacting via a vdW bond forming an angle $\varphi_{NGaN} = 71.8°$. Surprisingly, the angle φ_{NGaN} is less than 90° which would have been expected, since the two vdW σ bonds interact with two empty perpendicular p orbitals of $Ga^+(^1S)$. The bond lengths r_{N-N} and r_{Ga-N} are practically the same as in $GaN_2^+(\tilde{X}^1\Sigma^+)$ at all levels of theory (cf. Tables 1 and Figure 5). So, we expect that the MP2-optimized geometry for BSSE using the qz or aqz basis will be $r_{N-N} = 1.11$ and $r_{Ga-N} = 2.83$ Å, as in the case of $GaN_2^+(\tilde{X}^1\Sigma^+)$. The N≡N···Ga segment is quasi linear in all basis sets and methods with the calculated value of the angle at 174.7−179.6°. Natural population analysis (npa) shows that the N atom at the end loses about 0.18 e^- and the N closer to Ga gains about 0.16 e^-, leaving the Ga atom with a net positive charge of 0.98 e^-.

The calculated reaction energies for $GaN_4^+ \rightarrow Ga^+(^1S) + 2N_2(X^1\Sigma_g^+)$ and $GaN_4^+ \rightarrow GaN_2^+(\tilde{X}^1\Sigma^+) + N_2(X^1\Sigma_g^+)$ are 10.8 and 5.3 kcal/mol at the MP2-BSSE-corrected/qz level of theory (Table 3). The first one is twice as large as the second one; it is worth noting that the latter is similar to D_{e2} of $GaN_2^+(\tilde{X}^1\Sigma^+)$ that involves the removal of only one N_2 moiety at the same level of theory. In the case of GaN_2^+ the geometry was optimized for the BSSE energy, so judging from the similarity of the two systems, we can estimate that the BSSE-optimized energy of the GaN_4^+ for the above reactions will be 11.0 and 5.4 kcal/mol at the $MP2_{BSSE}$/qz or aqz level. The higher order of perturbation does not contribute significantly to the D_e of the above reactions; a single point calculation at the MP4/atz//MP2/atz level of theory gives D_e about 0.1 kcal/mol lower, and because the MP4 was not optimized we expect that the optimized MP4 values will be almost the same or a little bit larger than those of MP2. Finally, the B3LYP/LANL2DZ method gives reaction energies overestimated compared to MP2 values but in tolerable agreement (see Table 3).

Isomerization between two equivalent $\tilde{X}^1A_1$ minima, as the wedge changes direction, occurs via a transition state, the linear

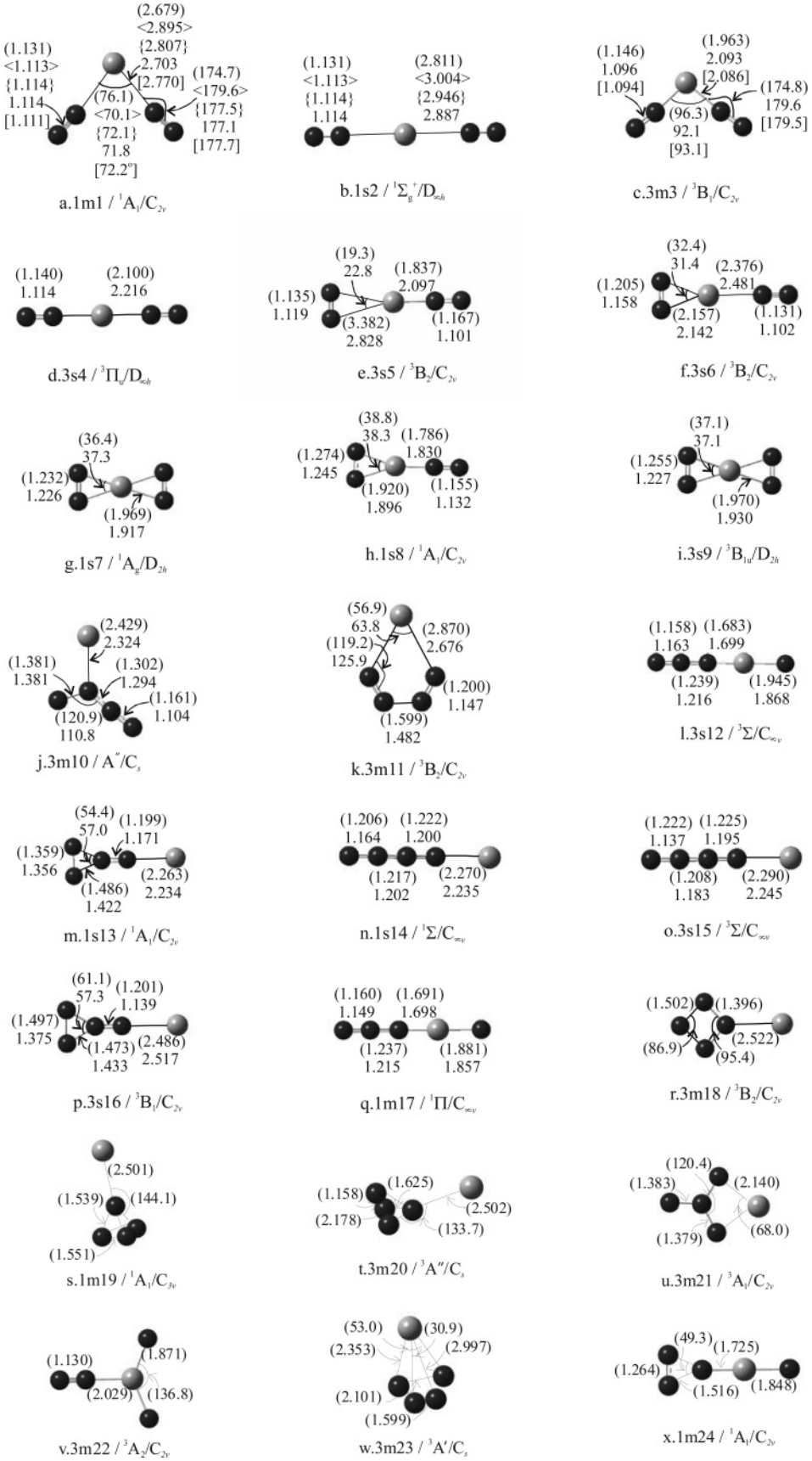

Figure 5. Optimized geometries of 24 structures of singlet and triplet GaN_4^+ species at (B3LYP/LANL2DZ) ⟨MP2/6-311G+(2df)⟩ {MP2/pVTZ} MP2/aug-cc-pVTZ [MP2/ cc-pVQZ] levels of theory, gray spheres ≡ Ga, black spheres ≡ N.

1s2 (Figure 5b), which has an increased r_{Ga-N} bond by ∼0.2 Å at the MP2/atz level of theory whereas the barrier to isomerization is 2.16 kcal/mol; see Table 3. Using the nonaugmented basis set cc-pVTZ, or the 6-311+G(2df) set, the calculated barrier is reduced substantially to 1.20 and 0.83 kcal/mol, respectively. The DFT value is 1.42 kcal/mol. The optimized

TABLE 3: GaN_4^+ Structures Absolute Energies E_e (hartree), Dissociation Energies and BSSE-Corrected Values D_e(BSSE) (kcal/mol), and Energy Differences ΔE (kcal/mol) at Different Levels of Theory

struct	method[a]	$-E_e$	D_{e1}(BSSE)[b] $GaN_4^+ \rightarrow Ga^+ + 4N$	D_{e2}(BSSE)[c] $GaN_4^+ \rightarrow Ga^+ + 2N_2$	D_{e3}(BSSE)[d] $GaN_4^+ \rightarrow GaN_2^+ + N_2$	D_{e3}(BSSE)[e] $GaN_4^+ \rightarrow Ga^+ + N_4$	ΔE
1m1	B3LYP		381.2 (377.7)	18.69 (13.08)	8.56 (5.80)		0.0
	MP2/6	2141.721597	470.4 (463.2)	10.67 (9.40)	5.28 (4.61)		0.0
	MP2/tz	2141.884764	470.0 (464.5)	12.55 (10.47)	6.18 (5.09)		0.0
	MP2/atz	2141.902498	474.8 (467.2)	13.62 (9.96)	6.88 (4.89)		0.0
	MP4/atz	2141.963891	459.5 (452.6)	13.45 (9.88)	6.73 (4.79)		0.0
	MP2/qz	2142.024649	483.6 (479.9)	12.98 (10.84)	6.42 (5.30)		0.0
1s2	B3LYP		379.8 (376.8)	17.26 (11.97)	7.14 (4.26)		1.42
	MP2/6	2141.720271	469.5 (463.8)	9.83 (8.61)	4.44 (3.77)		0.83
	MP2/tz	2141.882859	468.8 (463.6)	11.36 (9.62)	4.99 (4.09)		1.20
	MP2/atz	2141.899062	472.7 (466.5)	11.47 (9.31)	4.73 (3.78)		2.16
3m3	B3LYP		438.2 (434.0)	75.70 (66.04)	28.57 (23.85)		62.6
	MP2/atz	2141.772707	512.2 (498.6)	50.99 (41.37)	23.04 (17.55)		81.5
	MP2/qz	2141.883804	518.6 (512.8)	47.89 (43.53)	20.84 (18.50)		88.4
3s4	B3LYP		422.1 (418.5)	59.52 (50.60)	12.39 (7.37)		78.8
	MP2/atz	2141.756466	502.0 (491.3)	40.79 (33.97)	12.85 (9.92)		91.6
3s5	B3LYP		410.3 (406.2)	47.77 (40.88)	0.64 (−0.63) 22.23 (16.90)[f]		90.5
	MP2/atz	2141.740081	491.4 (481.8)	30.51 (24.57)	2.56 (1.07) 9.25 (5.06)[f]		101.9
3s6	B3LYP		402.2 (398.8)	39.63 (32.95)	−7.50 (−10.96) 14.09 (9.77)[f]		98.7
	MP2/atz	2141.738317	490.6 (480.1)	29.41 (22.58)	1.46 (−2.85) 8.14 (6.16)[f]		103.0
1s7	B3LYP		339.0 (334.5)[g]				161.8
	MP2/atz	2141.668257	446.7 (431.4)[g]				147.0
1s8	B3LYP		366.2 (361.1)[g]				134.6
	MP2/atz	2141.667817	446.4 (430.9)[g]				147.3
3s9	B3LYP		332.8 (328.4)				168.1
	MP2/atz	2141.627264	420.9 (407.2)				172.7
3m10	B3LYP		256.3 (253.3)[h]			14.24 (12.63)	125.0
	MP2/atz	2141.626542	301.7 (292.5)[h]			19.98 (15.42)	173.2
3m11	B3LYP		248.6 (245.4)[h]			10.95 (7.95)	132.7
	MP2/atz	2141.621067	298.3 (290.1)[h]			15.57 (12.28)	176.6
3s12	B3LYP		360.9 (355.1)				140.0
	MP2/atz	2141.609574	409.8 (397.0)				183.8
1s13	B3LYP		211.9 (209.0)			24.45 (23.29)	169.3
	MP2/atz	2141.607255	289.6 (279.2)			26.23 (21.27)	185.3
1s14	B3LYP		237.0 (234.0)			24.21 (22.14)	144.3
	MP2/6	2141.406738	272.8 (262.5)				197.6
	MP2/tz	2141.582878	280.6 (272.7)				189.4
	MP2/atz	2141.603920	287.5 (276.4)			24.43 (19. 20)	187.4
3s15	B3LYP		262.0 (259.2)[h]			21.86 (19.74)	119.3
	MP2/atz	2141.600206	285.2 (274.6)[h]			22.98 (17.79)	189.7
3s16	B3LYP		199.9 (197.3)[h]			11.56 (9.83)	181.4
	MP2/atz	2141.537180	245.4 (237.3)[h]			7.77 (4.70)	229.2
1m17	B3LYP		314.5 (309.1)[g]				186.4
	MP2/atz	2141.533607	353.2 (348.1)[g]				231.5
3m18	B3LYP		312.7 (309.9)				188.2
1m19	B3LYP		187.1 (183.7)				194.1
3m20	B3LYP		288.1 (285.2)				212.8
3m21	B3LYP		285.1 (281.5)				215.7
3m22	B3LYP		284.7 (280.7)				216.2
3m23	B3LYP		281.4 (277.3)				219.5
1m24	B3LYP		122.3 (117.5)				258.9

[a] B3LYP = B3LYP/LANL2DZ, MP2/6 = MP2/6-311+G(2df), MP2/tz = MP2/cc-pVTZ, MP2/atz = MP2/aug-cc-pVTZ, and MP2/qz = MP2/cc-pVQZ. The unrestricted MP method has been used for the triplet structures. [b] D_e with respect to $Ga^+(^1S$ and $^3P) + 4N(^4S)$ for the singlet and triplet states, respectively. [c] D_e with respect to $Ga^+(^1S$ and $^3P) + 2N_2(X^1\Sigma_g^+)$ for the singlet and triplet states, respectively. [d] D_e with respect to $GaN_2^+(\tilde{X}^1\Sigma^+$ and $\tilde{X}^3\Pi) + N_2(X^1\Sigma_g^+)$ for the singlet and triplet states, respectively. [e] D_e with respect to $N_4(^3A'') + Ga^+(^1S)$ for 3m10, $N_4(^3B_2) + Ga^+(^1S)$ for 3m11, $N_4(^1A_1) + Ga^+(^1S)$ for 1s13, $N_4(^1\Sigma) + Ga^+(^1S)$ for 1s14, $N_4(^3\Sigma) + Ga^+(^1S)$ for 3s15, and $N_4(^3B_1) + Ga^+(^1S)$ for 3s16. [f] D_e with respect to $GaN_2^+(\tilde{b}\ ^3B_2) + N_2(X^1\Sigma_g^+)$. [g] D_e with respect to $Ga^+(^3P) + 4N(^4S)$; the D_e BSSE corrected with respect to $Ga^+(^1S) + 4N(^4S)$ is 312.6 (1s7), 312.1 (1s8), and 229.3 kcal/mol (1m17) at the MP2/atz level. [h] D_e with respect to $Ga^+(^1S) + 4N(^4S)$.

MP2/atz potential energy profiles of the 1m1($^1A_1$) and 1s2($^1\Sigma_g^+$) structures of the GaN_4^+ cation are plotted as the Ga^+ is being removed in Figure 6. In the inset, the optimized potential energy profile of the ground state, 1m1($^1A_1$) - 1s2($^1\Sigma_g^+$) with respect to the angle φ is shown, and a contour plot of the optimized two-dimensional potential energy surface between the two 1m1-($^1A_1$) minima and their transition state 1s2($^1\Sigma_g^+$) at the MP2/atz level is given in Figure 7.

Table 4 presents harmonic frequencies of 1m1 and 1s2 at MP2/tz and MP2/atz level of theory. The frequencies ω_2 to ω_6 (1m1) and ω_3 to ω_8 (1s2) are all within a narrow range of 20 cm^{-1}; consequently, the ordering of frequencies of stretching

TABLE 4: Harmonic Frequencies (cm^{-1}) and IR Intensities (km/mol) of the Six Singlet and Eight Triplet Structures of GaN_4^+ Cation at MP2/cc-pVTZ(tz) and MP2/aug-cc-pVTZ(atz) Level of Theory

	1m1				1s2				3m3		3s4	
	tz		atz		tz		atz		atz		atz	
	ω_e	IR	ω_e	IR	ω_e	IR	ω_e	IR	ω_e	IR	ω_e	IR
ω_1	34.1	0.7	37.3	1.1	7.8i	2.3	16.6i	2.1	68.4	0.3	86.1i	0.7
ω_2	90.9	12.5	86.6	0	7.8i	2.3	16.6i	2.1	221.7	1.2	48.0	0.3
ω_3	98.8	21.3	88.6	0.02	81.9	0	63.2	47.2	261.1	5.3	125.5	2.3
ω_4	109.1	1.3	93.0	2.8	86.7	42.2	78.6	0	261.2	0	153.8	0
ω_5	110.3	0	96.9	12.9	99.1	0.1	78.6	0	261.4	1.3	190.5	0
ω_6	111.2	0.05	100.4	23.2	99.1	0.1	79.0	0	264.0	0.0002	227.4	0
ω_7	133.4	6.5	137.5	8.7	99.5	0	84.2	0	288.3	6.6	274.9	154.3
ω_8	2189.1	23.1	2178.8	27.1	99.5	0	84.2	0	3528.9	357.5	286.8	2.2
ω_9	2189.8	14.7	2179.8	17.6	2192.4	30.6	2182.1	33.8	3572.0	872.8	2378.6	0.0001
ω_{10}					2192.7	0	2182.6	0			2450.6	1471

	3s5		3s6		1s7		1s8		3s9		3m10	
	atz		atz		atz		atz		atz		atz	
	ω_e	IR	ω_e	IR	ω_e	IR	ω_e	IR	ω_e	IR	ω_e	IR
ω_1	34.9i	0.2	119.9i	0.05	73.3i	4.3	330.5i	51.8	228.5i	0	70.7	0.3
ω_2	24.1i	0.2	27.6i	0.9	55.8	16.1	58.8	9.7	75.4	23.1	105.0	0.1
ω_3	68.1	14.0	13.6i	0.7	218.7	0	214.4	18.8	209.0	40.4	162.0	45.4
ω_4	91.1	0.2	117.0	35.6	506.1	0	293.3	1.2	520.6	0	292.7	12.2
ω_5	218.2	0.6	139.6	1.6	557.8	0	428.8	177.4	682.7	101.1	638.8	10.2
ω_6	268.0	14.1	447.9	171.4	586.9	3.5	573.1	258.4	1579.2	0.001	671.6	3.1
ω_7	289.6	0.1	451.7	7.8	732.7	106.1	659.9	0.8	1596.7	0	940.8	92.3
ω_8	2137.5	0.3	2505.0	3403	1487.2	0	1365.7	902.9	1827.3	18902	1057.4	252.6
ω_9	3441.3	1168	3248.0	1045	1658.5	218.5	1920.3	1255	11244	0.001	3451.9	16.11

	3m11		3s12		1s13		1s14			
	atz		atz		atz		tz		atz	
	ω_e	IR	ω_e	IR	ω_e	IR	ω_e	IR	ω_e	IR
ω_1	43.7	4.4	197.2i	13.0	180.6i	2.9	810.8i	0.0007	795.3i	0.04
ω_2	110.0	25.3	197.2i	13.0	29.7i	4.1	43.9i	2.7	47.1i	2.7
ω_3	151.4	1.1	92.9	9.6	68.3	0.9	55.0	0.04	44.7	0.03
ω_4	283.4	0	92.9	9.6	185.1	82.2	168.5	94.4	188.2	92.6
ω_5	297.1	0.4	455.2	0.9	497.9	6.9	264.6	6.6	262.7	6.9
ω_6	607.9	13.4	455.2	0.9	609.5	44.5	292.3	7.8	288.6	7.9
ω_7	1060.8	6.7	525.3	22.4	894.7	13.0	627.9	0.0001	631.4	0.002
ω_8	2440.8	208.0	762.6	21.3	1022.3	10.9	1016.7	144.0	1020.7	147.4
ω_9	5798.3	10146	1661.7	574.3	1894.5	797.5	1744.4	512.3	1743.9	533.6
ω_{10}			2805.5	423.3			2407.6	88.0	2402.2	90.8

and bending modes is different in the two basis sets. Compared to the frequencies of the modes of $GaN_2^+(\tilde{X}^1\Sigma^+)$ and N_2, they show small shifts ranging from -33 to $+34$ cm^{-1}. The two imaginary frequencies of 1s2 correspond to the bending of the linear N−N−Ga^+−N−N in two dimensions.

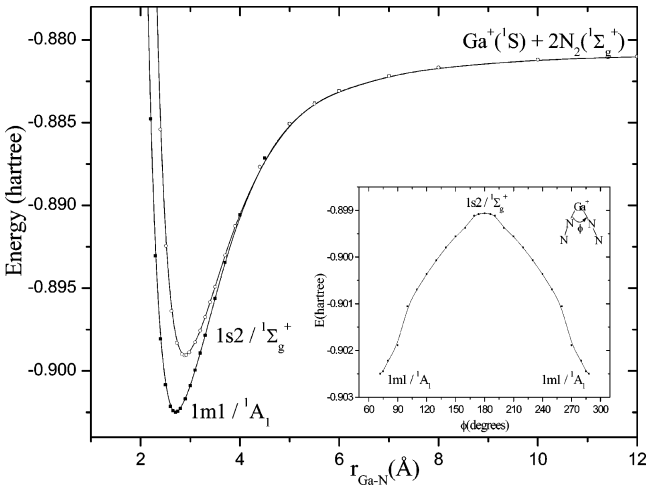

Figure 6. Potential energy curves of the $1m1(^1A_1)$ and $1s2(^1\Sigma_g^+)$ states of the GaN_4^+ cation with respect to the r_{Ga-N} distance, at the MP2/aug-cc-pVTZ level of theory. Inset: Optimized potential energy profile of $1m1(^1A_1)-1s2(^1\Sigma_g^+)$ with respect to the angle φ.

The second minimum calculated for GaN_4^+ is the $3m3(^3B_1)$ structure (Figure 5c) which is a bent structure similar to 1m1, but here the Ga^+ cation is in its first excited state ^3P, so its components are $Ga^+(^3P) + 2N_2(X^1\Sigma_g^+)$ or $GaN_2^+(\tilde{a}^3\Pi) + N_2(X^1\Sigma_g^+)$. In this case, the angle φ_{NGaN} is 92.1°, about 20° larger than that of 1m1. The two N_2 are perpendicular to each other because they bind to two empty perpendicular p orbitals of Ga^+. The reaction energies are 43.5 and 18.5 kcal/mol, respectively, for the two dissociation process given above at the MP2-BSSE corrected/qz level of theory (Table 3), and we can estimate that the BSSE-optimized energy will be 43.7 and 18.6 kcal/mol at the $MP2_{BSSE}$/qz or aqz level. These values are about 4 times higher than the corresponding values calculated for 1m1. The Ga^+−N bonds of 3m3 are much shorter than those of 1m1, and they are not vdW bonds as in the case of 1m1. The spin contamination of UMP2 calculation is very small, with $\langle S^2\rangle = 2.02$ instead of 2.

The transition state between the two equivalent wedge 3m3 structures is the linear 3s4 species (Figure 5d). The energy barrier to inversion is 10.2 kcal/mol. Note that the DFT method overestimates this barrier by 6 kcal/mol (see Table 3). In Figure 8, the MP2/atz potential energy profiles of the $3m3(^3B_1)$ and $3s4(^3\Pi_u)$ states of the GaN_4^+ cation are plotted as the Ga^+ is being removed while the angle φ_{NGaN} is kept constant. In the inset, the optimized potential energy profile of $3m3(^3B_1)-3s4(^3\Pi_u)$ with respect to the angle φ is drawn; a

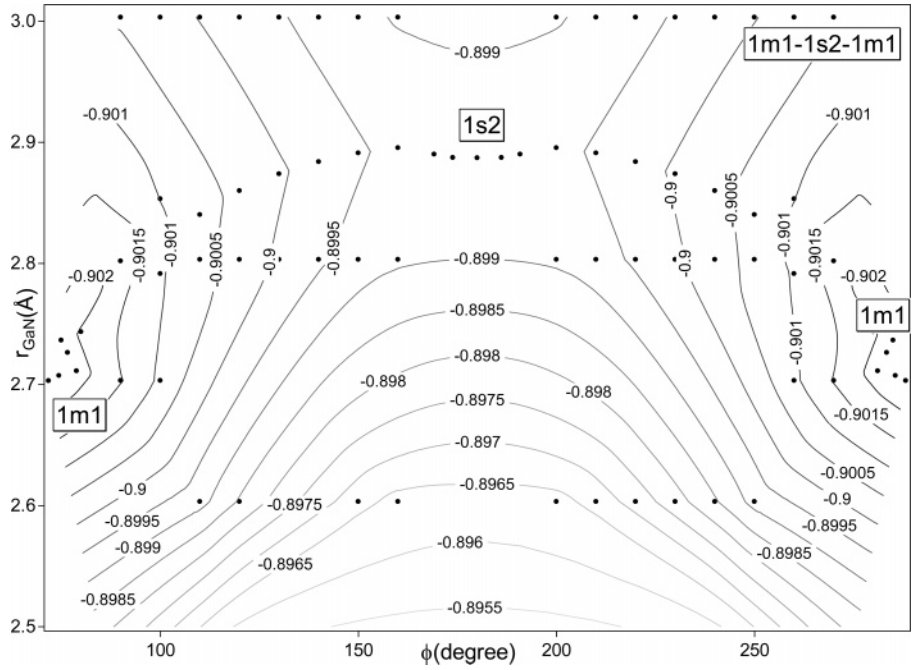

Figure 7. Potential energy surface of $1m1(^1A_1)-1s2(^1\Sigma_g^+)$ as a function of the Ga−N distance and the φ_{NGaN} angle represented by contour lines equally spaced by 0.0002 hartree at the MP2/aug-cc-pVTZ level of theory. The contour lines were drawn on the basis of the data calculated at the coordinates represented by the filled circles.

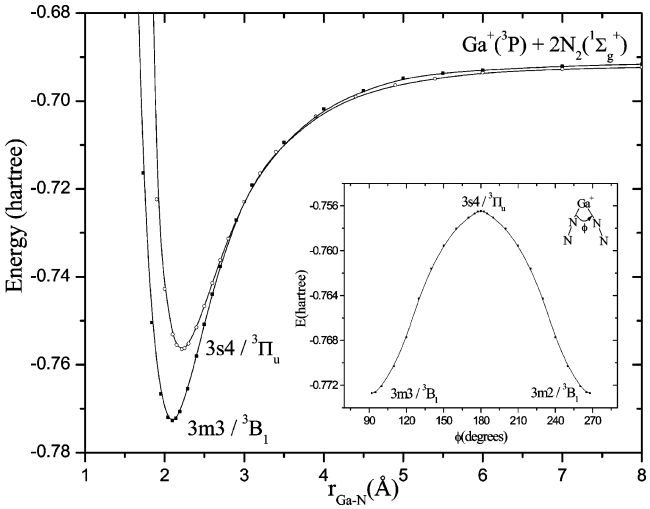

Figure 8. Potential energy curves of the $3m3(^3B_1)$ and $3s4(^3\Pi_u)$ states of the GaN_4^+ cation with respect to the r_{Ga-N} distance, at the MP2/aug-cc-pVTZ level of theory. Inset: Optimized potential energy profile of $3m3(^3B_1)-3s4(^3\Pi_u)$ with respect to the angle φ.

contour plot of the potential energy surface showing the two $3m3(^3B_1)$ minima and their transition state $3s4(^3\Pi_u)$ is given in Figure 9.

Comparing the modes of 3m3 to those of $GaN_2^+(\tilde{a}^3\Pi)$ and N_2, the ω_2 to ω_7 frequencies of 3m3 are shifted only by about $\pm$ 20 cm^{-1}. The corresponding ω values of 3s4 are much more red-shifted, up to 110 cm^{-1}. The ω_8 (3m3, symmetric stretch of two N≡N) presents a large blue shift of 1343 cm^{-1} with respect to the free N_2, similar to the 1338 cm^{-1} shift in $GaN_2^+(\tilde{a}^3\Pi)$, whereas ω_9 (3m3), which corresponds to asymmetric stretch, shows an even larger shift of 1386 cm^{-1}. The large blue shifts results from the fact that the N_2 is more rigid and cannot stretch freely. In 3s4 the ω_8 and ω_9 are blue-shifted only by 192 and 264 cm^{-1}, which is consistent with the fact that the Ga−N bond is elongated compared to 3m3 and N_2 has more freedom to stretch.

In 3m3 the natural population analysis shows that electrons are transferred to the Ga^+ cation whose net charge is $+0.88|e^-|$, the N atoms at the end have a positive charge of about +0.28 each, and the N atoms closer to Ga have gained 0.22 e^-. A similar charge transfer exists in the 3s4 structure.

The $3s5(^3B_2)$, $3s6(^3B_2)$, and $1s8(^1A_1)$ structures (Figures 5e,f,h) lie at 20.5, 21.6, and 65.8 kcal/mol, respectively, above the lowest triplet structure, 3m3. They are T-shaped and have very similar shapes consisting of either a triangular GaN_2^+ and a N_2 connected with a bond to Ga^+, or a linear Ga^+NN whose Ga^+ interacts with the N_2 triple bond. Although both triplet structures 3s5 and 3s6 may be thought of as consisting of $N_2(X^1\Sigma_g^+) + GaN_2^+(^3\Pi)$ or $GaN_2^+(^3B_2) + N_2(X^1\Sigma_g^+)$, they differ in the actual values of the bond-lengths and, in fact, the $N_2(X^1\Sigma_g^+) + GaN_2^+(^3\Pi)$ limit is more appropriate for 3s5 with a BSSE-corrected dissociation energy $D_{e3}(BSSE) = 1.1$ kcal/mol and the $GaN_2^+(^3B_2) + N_2(X^1\Sigma_g^+)$ limit for 3s6 with $D_{e3}(BSSE) = 6.2$ kcal/mol. The optimized PEP of 3s5 and 3s6 structures are drawn as the N_2 is removed in Figure 10. The npa shows that in 3s5 Ga^+ gains about 0.1 e^-. The GaN_2^+ species of the singlet $1s8(^1A_1)$ is a highly excited state that has not been calculated here. The structure 1s8 has significantly smaller r_{Ga-N} distances than those of $\tilde{X}^1\Sigma^+$ and $\tilde{A}^1A_1$ of GaN_2^+, by more than 1 Å (Table 1, Figure 5h). In this structure Ga^+ is in the excited ^3P state and the distance r_{Ga-N} does not indicate a vdW bond.

The $1s7(^1A_g)$ and $3s9(^3B_{1u})$ are both transition states of D_{2h} symmetry (Figure 5 and Table 4). Both states, singlet and triplet, contain $Ga^+(^3P)$ and have $r_{Ga-N} = 1.92$ Å, $r_{N-N} = 1.13$ Å and $\varphi_{NGaN} = 37°$, at the MP2/atz level of theory.

The $3m10(A'')$ and $3m11(^3B_2)$ minima are an open and a cyclic structure, respectively (cf. Figure 5), having a triplet N_4 species, $^3A''$ and $^3B_1$, respectively, interacting with a singlet $Ga^+(^1S)$. The MP2 BSSE-corrected dissociation energy with respect to $N_4 + Ga^+$ is 15.4 and 12.3 kcal/mol at MP2(BSSE)/atz level of theory. The r_{GaN} bond is 2.32 and 2.68 Å, respectively. In 3m10 the npa shows that there is a reallocation

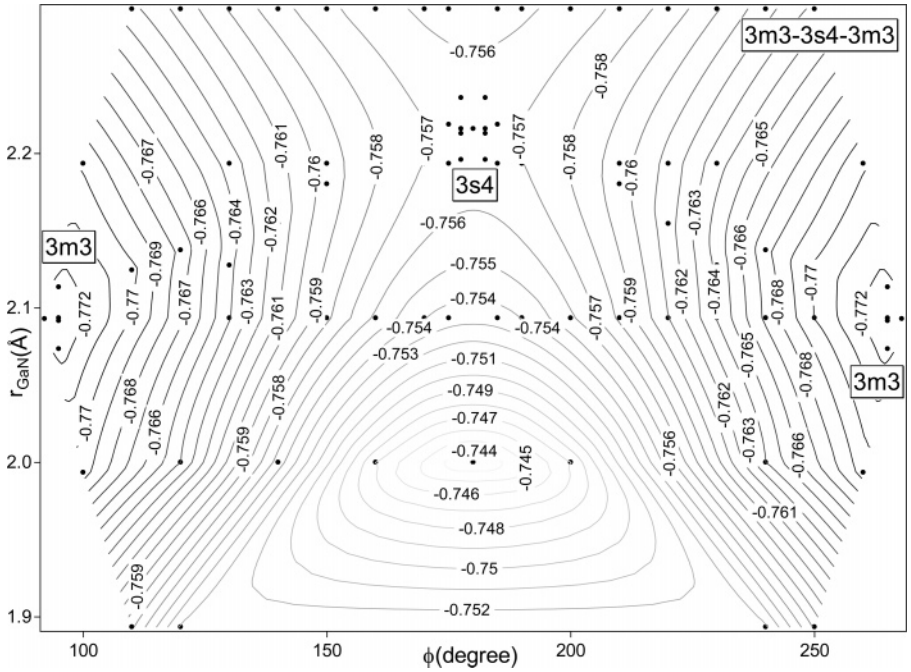

Figure 9. Potential energy surface of $3m3(^3B_1)-3s4(^3\Pi_u)$ as a function of the Ga−N distance and the ∠NGaN angle represented by contour lines equally spaced by 0.001 hartree at the MP2/aug-cc-pVTZ level of theory. The contour lines were drawn on the basis of the data calculated at the coordinates represented by the filled circles.

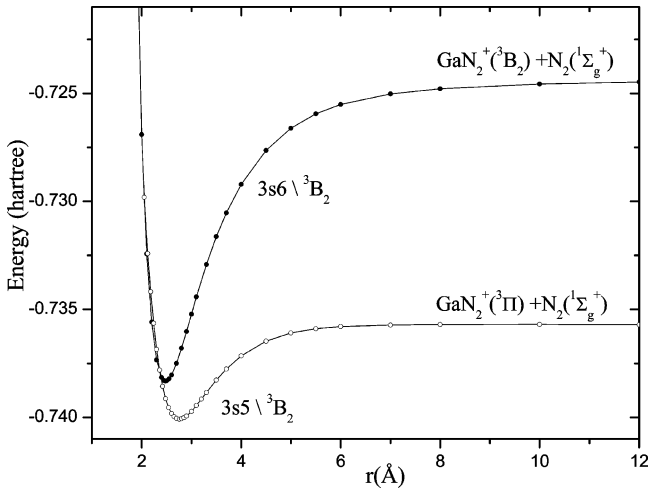

Figure 10. Potential energy curves of the $3s5(^3B_2)$ and $3s6(^3B_2)$ states of the GaN_4^+ cation with respect to the r_{Ga-N} and the $r_{Ga-\equiv}$ distance, respectively at the MP2/aug-cc-pVTZ level of theory.

of charge, i.e., $Ga^{+0.97}N_1^{+0.15}N_2^{-0.62}N_3^{+0.25}N_4^{+0.24}$ (Ga^+ is bonded to N_2).

The linear structures N−N−N−Ga−N^+, $3s12(^3\Sigma)$ and $1m17(^1\Pi)$, both have $Ga^+(^3P)$ and the r_{Ga-N} bonds are ∼1.86 and 1.70 Å for the Ga−N bond at the end and for the bond in the middle in both structures. The 3s12 at the DFT level is predicted to be a minimum, but in MP2/atz it is a saddle point. In this study, for most of the electronic states calculated, the DFT method predicts the same minima as MP2/atz, but there are some exceptions, as for example the case of 3s12.

The next electronic structures discussed, a singlet $1s13(^1A_1)$ and a triplet $3s16(^3B_1)$ (Figure 5m,p), contain the N_4 moiety, which is formed from a triangular N_3 and a single N atom, giving rise to a singlet $N_4(^1A_1)$ and a triplet $N_4(^3B_1)$ structure, respectively. A singlet $Ga^+(^1S)$ is connected to N via a bond of 2.234 and 2.517 Å, respectively. The reaction energies of 1s13 → $N_4(^1A_1)$ + $Ga^+(^1S)$ and 1s16 → $N_4(^3B_1)$ + $Ga^+(^1S)$ are 21.3 and 4.7 kcal/mol, respectively.

The last structures examined at the MP2/atz level are the linear $1s14(^1\Sigma)$ and $3s15(^3\Sigma)$ having a linear $N_4(^1\Sigma)$ and $N_4(^3\Sigma)$ + $Ga^+(^1S)$, respectively. The r_{GaN} bond is 2.24 Å, and the binding energies are 19.2 and 17.8 kcal/mol, respectively. In the 1s14 electronic state the MP2/6-311G+(2df) calculation gives shorter bonds compared to the MP2/atz level; on the contrary, in the 1m1 and 1s2 by the former method the r_{GaN} was elongated (Figure 5).

The next seven electronic states shown in Figure 5 are calculated only with the DFT method. Judging from the first 17 electronic structures, where the geometries in B3LYP/LANL2DZ were in good agreement even with a small basis set with the MP2/atz level of theory, the next seven structures calculated only in DFT are expected to have similar geometries at the MP2/atz level, yet the energy ordering of these structures may change in an MP2 calculation, as can be seen in Table 3 for the first 17 structures were calculated in both MP2 and B3LYP methods.

V. Synopsis and Remarks

Gallium nitrides are semiconducting materials with promising technological applications in microelectronics and optics, so the information on the geometry and electronic structure of small GaN clusters is essential for both basic knowledge and technological applications. In the present work employing density functional theory (B3LYP/LANL2DZ) and perturbation theory (MP2, MP4/aug-cc-pVxZ, x = T, Q) the gallium dinitride cation, GaN_2^+, and the gallium tetranitride cation, GaN_4^+, were systematically examined for the first time. A total of 7 (GaN_2^+) and 24 (GaN_4^+) electronic structures were examined. Their geometries, dissociation energies, and harmonic frequencies are reported, and potential energy profiles, potential energy surfaces, and the bonding mechanisms of some lowest states are given. Our findings can be summarized as follows.

1. The ground state of GaN_2^+ ($\tilde{X}^1\Sigma^+$) is a linear van der Waals molecule N≡N···Ga^+ with r_{Ga-N} = 2.829 Å and dissociation energy of 5.6 kcal/mol with respect to $Ga^+(^1S)$ + $N_2(X^1\Sigma_g^+)$

products. The Ga^+ cation has to overcome a barrier of 4.3 kcal/mol to shift from one N atom to the other one.

2. The next minimum is the $\tilde{a}^3\Pi$ state ($NNGa^+$, $r_{Ga-N} = 2.067$ Å), and the reaction energy of $GaN_2^+(\tilde{a}^3\Pi) \rightarrow Ga^+(^3P) + N_2(X^1\Sigma_g^+)$ is 24.8 kcal/mol. On this potential energy surface, a local minimum 1^3B_2 is found at 7.4 kcal/mol above the $\tilde{a}^3\Pi$ state, and a barrier of 9 kcal/mol has to be overcome to shift to the $\tilde{a}^3\Pi$ structure.

3. The ground electronic state of GaN_4^+ is a triangular structure of $^1A_1(C_{2v})$ symmetry with a D_e of 11.0 and 5.4 kcal/mol with respect to $Ga^+(^1S) + 2N_2(X^1\Sigma_g^+)$ and $GaN_4^+ \rightarrow GaN_2^+(\tilde{X}^1\Sigma^+) + N_2(X^1\Sigma_g^+)$, respectively. The energy of isomerization between two equivalent $\tilde{X}^1A_1$ as the wedge changes direction via a linear state (N−N−Ga^+−N−N), is 2.2 kcal/mol.

4. The first excited state of GaN_4^+ is also a triangular structure of $^3B_1(C_{2v})$ symmetry with a $D_e = 43.7$ and 18.6 kcal/mol with respect to $Ga^+(^3P) + 2N_2(X^1\Sigma_g^+)$ and $GaN_2^+(\tilde{a}^3\Pi) + N_2(X^1\Sigma_g^+)$, respectively. The energy of isomerization of $\tilde{a}^3B_1 \leftarrow$ linear N−N−Ga^+−N−N $\rightarrow \tilde{a}^3B_1$ is 10.2 kcal/mol.

5. The third ($^3A''$) and the fourth ($^3B_2$) minima are an open and a cyclic structure, respectively, having a triplet N_4 structure. The dissociation energy with respect to $N_4 + Ga^+$ is 15.4 and 12.3 kcal/mol.

6. The B3LYP/LANL2DZ and MP2/aug-cc-pVTZ geometries were in fair agreement. But the energy ordering of some structures is not the same in the two methods, resulting in some DFT reactions energies to be significantly overestimated with respect to MP2 data for both GaN_2^+ and GaN_4^+. Moreover, 2 structures out of 17, i.e., 3m11 and 3s12, which are a minimum and a saddle point at the MP2/atz level, respectively, are characterized as a saddle point and a minimum in the B3LYP method.

Acknowledgment. Financial support has been provided by the Greek General Secretariat for Research and Technology through a Greece−Slovakia bilateral collaboration program.

Supporting Information Available: The optimized geometries of 10 high lying structures of singlet and triplet GaN_4^+ species at B3LYP/LANL2DZ level of theory are provided. This material is available free of charge via the Internet at http://pubs.acs.org.

References and Notes

(1) Goldberger, J.; He, R.; Zhang, Y.; Lee, S.; Yan, H.; Choi, H. J.; Yang, P. *Nature* **2003**, *422*, 599.

(2) Nakamura, S. *Science* **1998**, *281*, 956.

(3) Waltereit, P.; Brandt, O.; Trampert, A.; Grahn, H. T.; Menniger, J.; Ramsteiner, M.; Reiche, M.; Ploog, K. H. *Nature* **2000**, *406*, 865.

(4) For example, Fuchs, M.; Da Silva, J. L. F.; Stampfl, C.; Neugebauer, J.; Scheffler, M. *Phys. Rev. B* **2002**, *65*, 245212.

(5) BelBruno, J. J. *Heteroat. Chem.* **2000**, *11*, 281.

(6) Kandalam, A. K.; Blanco, M. A.; Pandey, R. *J. Phys. Chem. B* **2001**, *105*, 6080; **2002**, *106*, 1945.

(7) Denis, P. A.; Balasubramanian, K. *Chem. Phys. Lett.* **2006**, *423*, 247.

(8) M. Urban and I. Cernusak, personal communication, work in progress.

(9) Kandalam, A. K.; Pandey, R.; Blanco, M. A.; Costales, A.; Recio, J. M.; Newsam, J. M. *J. Phys. Chem. B* **2000**, *104*, 4361.

(10) Wang, C. S.; Balasubramanian, K. *Chem. Phys. Lett.* **2004**, *404*, 294.

(11) Tzeli, D.; Petsalakis, I.; Theodorakopoulos, G. To be submitted for publication.

(12) Zhou, M.; Andrews, L. *J. Phys. Chem. A* **2000**, *104*, 1648.

(13) Song, B.; Cao, P. L. *Phys. Lett. A* **2004**, *328*, 364.

(14) Wang, C.-S.; Balasubramanian, K. *Chem. Phys. Lett.* **2004**, *404*, 294.

(15) Becke, A. D. *J. Chem. Phys.* **1993**, *98*, 1372.

(16) Lee, C.; Yang, W.; Parr, R. G. *Phys. Rev. B* **1988**, *37*, 785.

(17) Hay, P. J.; Wadt, W. R. *J. Chem. Phys.* **1985**, *82*, 299.

(18) Dunning, T. H., Jr. *J. Chem. Phys.* **1989**, *90*, 1007. Wilson, A. K.; Woon, D. E.; Peterson, K. A.; Dunning, T. H., Jr. *J. Chem. Phys.* **1999**, *110*, 7667.

(19) Pople, J. A. *J. Chem. Phys.* **1980**, *72*, 650. Curtiss, L. A.; McGrath, M. P.; Blandeau, J. P.; Davis, N. E.; Binning, R. C. Radom, L., Jr. *J. Chem. Phys.* **1995**, *103*, 6104.

(20) Boys, S. F.; Bernardi, F. *Mol. Phys.* **1970**, *19*, 553. Liu, B.; Mclean, A. D. *J. Chem. Phys.* **1973**, *59*, 4557. Jansen, H. B.; Ros, P. *Chem. Phys. Lett.* **1969**, *3*, 140.

(21) Jeziorski, B.; Moszynski, R.; Szalewicz, K. *Chem. Rev.* **1994**, *94*, 1887.

(22) Frisch, M. J.; Trucks, G. W.; Schlegel, H. B.; Scuseria, G. E.; Robb, M. A.; Cheeseman, J. R.; Montgomery, J. A.; Vreven, T.; Kudin, K. N.; Burant, J. C.; Millam, J. M.; Iyengar, S. S.; Tomasi, J.; Barone, V.; Mennucci, B.; Cossi, M.; Scalmani, G.; Rega, N.; Petersson, G. A.; Nakatsuji, H.; Hada, M.; Ehara, M.; Toyota, K.; Fukuda, R.; Hasegawa, J.; Ishida, M.; Nakajima, T.; Honda, Y.; Kitao, O.; Nakai, H.; Klene, M.; Li, X.; Knox, J. E.; Hratchian, H. P.; Cross, J. B.; Adamo, C.; Jaramillo, J.; Gomperts, R.; Stratmann, R. E.; Yazyev, O.; Austin, A. J.; Cammi, R.; Pomelli, C.; Ochterski, J. W.; Ayala, P. Y.; Morokuma, K.; Voth, G. A.; Salvador, P.; Dannenberg, J. J.; Zakrzewski, V. G.; Dapprich, S.; Daniels, A. D.; Strain, M. C.; Farkas, O.; Malick, D. K.; Rabuck, A. D.; Raghavachari, K.; Foresman, J. B.; Ortiz, J. V.; Cui, Q.; Baboul, A. G.; Clifford, S.; Cioslowski, J.; Stefanov, B. B.; Liu, G.; Liashenko, A.; Piskorz, P.; Komaromi, I.; Martin, R. L.; Fox, D. J.; Keith, T.; Al-Laham, M. A.; Peng, C. Y.; Nanayakkara, A.; Challacombe, M.; Gill, P. M. W.; Johnson, B.; Chen, W.; Wong, M. W.; Gonzalez, C.; Pople, J. A., Jr. *Gaussian 03*, revision C.02; Gaussian, Inc.: Wallingford CT, 2004.

(23) Werner, H.-J.; Knowles, P. J.; Lindh, R.; Manby, F. R.; Schütz, M.; Celani, P.; Korona, T.; Rauhut, G.; Amos, R. D.; Bernhardsson, A.; Berning, A.; Cooper, D. L.; Deegan, M. J. O.; Dobbyn, A. J.; Eckert, F.; Hampel, C.; Hetzer, G.; Lloyd, A. W.; McNikolas, S. J.; Meyer, W.; Mura, M. E.; Nicklass, A.; Palmieri, P.; Pitzer, R.; Schumann, U.; Stoll, H.; Stone, A. J.; Tarroni, R.; Thorsteinsson, T. *MOLPRO 2006.1*, a package of ab initio programs.